Biochemical Pharmacology 175 (2020) 113915

Contents lists available at ScienceDirect

Biochemical Pharmacology

journal homepage: www.elsevier.com/locate/biochempharm

Necroptosis mediated by impaired autophagy flux contributes to adverse ventricular remodeling after myocardial infarction

Haining Zhang[a,1,*], Yuan Yin[b,1], Yumei Liu[c], Gangling Zou[d], Hao Huang[a], Peipei Qian[a], Guiping Zhang[a], Jinxin Zhang[e,*]

[a] Department of Pharmacology, School of Pharmaceutical Sciences and the Fifth Affiliated Hospital, Guangzhou Medical University, Guangzhou 511436, PR China
[b] Affiliated Guangxi International Zhuang Medical Hospital, Guangxi University of Traditional Chinese Medicine, Nanning 530021, PR China
[c] Medical College of Jiaying University, Meizhou 514031, PR China
[d] Nanhai Mental Health Center, People's Hospital of Nanhai District, Foshan 528200, PR China
[e] Department of Medical Statistics and Epidemiology, School of Public Health, Sun Yat-sen University, Guangzhou 510080, China

ARTICLE INFO

Keywords:
Myocardial ischemia
Loss of cardiomyocytes
Necroptosis
RIP3
Autophagy
Cardiac remodeling

ABSTRACT

Loss of functional cardiomyocytes by cell death after myocardial infarction is most critical for the subsequent left ventricular remodeling, cardiac dysfunction and heart failure. Numerous studies have implicated that dysregulation of autophagy might contribute to cardiomyocyte death. However, the underlying mechanisms by which autophagy dysregulation-mediated cell death remains to be elusive. Herein, we showed that, in response to myocardial ischemic damage *in vivo* and *in vitro*, autophagy activity was increased quickly but followed by the process of impaired autophagic degradation as evidenced by the sustained higher level of beclin1 until 12 weeks after myocardial infarction, while, increased accumulation of LC3 and p62. The results from both tandem mRFP-GFP-LC3 adenovirus and lysosomal inhibitor chloroquine supported defective autophagy induction by ischemia injury. Importantly, we found that the impaired autophagy flux, induced not only pharmacologically by CQ but also genetically by beclin1 knockdown, upregulated the expression of RIP3 and aggravated OGD-induced necroptotic cardiomyocyte death and cardiac dysfunction. While, upregulation of autophagy by cardiac-specific beclin1 overexpression partially ameliorated cardiac dysfunction after MI. Furthermore, constitutive activation of necroptosis by forced cardiac-specific overexpression of RIP3 aggravated necrotic cardiomyocyte death, post-MI cardiac remodeling and cardiac dysfunction, but all of which could be ameliorated by inhibition of necroptosis by RIP3 knockdown. In conclusion, these results suggested that autophagy dysfunction-mediated necroptosis mechanistically contributed to loss of cardiomyocytes, adverse ventricular remodeling and progressive heart failure after myocardial Infarction. Inhibition of necroptosis might be the potential target for preventing post-infarction cardiac remodeling and heart failure.

1. Introduction

Myocardial infarction (MI) is a common complication of coronary artery disease and the leading cause of death worldwide [1]. Following MI, maladaptive cardiac remodeling with sustained loss of cardiomyocytes by cell death accounts for the deteriorated cardiac performance and ultimately clinical heart failure or sudden death. Despite recent advances in treatment and increased availability of heart transplants, the progressive heart failure after MI remains challenging to be treated, and approximately half of the patients that developed heart failure die within 5 years of diagnosis [2]. Therefore, the development of new therapeutically promising strategies to prevent the loss of cardiomyocytes and cardiac remodeling after myocardial infarction is potentially amenable for control and therapeutic intervention of heart failure.

It is increasingly apparent that autophagy, as a lysosome-dependent degradation pathway, plays indispensable roles in the maintenance of cardiac homoeostasis and performance by preventing accumulation of damaged proteins and organelles, either under normal condition or in response to stresses such as nutrient deprivation, growth factor withdrawal, hypoxia, and infection [3]. As such, autophagy machinery is functionally protective from cell death and supports cell survival especially under stressful conditions. However, accumulating evidence revealed that the excessive or insufficient autophagic activity can each

* Corresponding authors.
E-mail addresses: zhanghn@gzhmu.edu.cn (H. Zhang), zhjinx@mail.sysu.edu.cn (J. Zhang).
[1] Haining Zhang and Yuan Yin contributed equally to this work.

https://doi.org/10.1016/j.bcp.2020.113915
Received 22 October 2019; Accepted 11 March 2020
Available online 14 March 2020
0006-2952/

contribute to cell death either in autophagic cell death, or apoptosis, or in non-apoptotic, including necrotic cell death [4], which might be associated with the pathogenesis of cardiovascular diseases, including heart failure [5,6], hypertrophic and dilated cardiomyopathy and ischemic heart disease [7,8]. But to date, it remains controversial over the role of autophagy in post-MI cardiac remodeling. Also, the underlying mechanism by which the dysregulated autophagy involved in cell death under conditions of ischemic stress has not been fully characterized.

Numerous studies have demonstrated that necrotic cardiomyocyte death induced by acute myocardial infarction is an important component in the loss of cardiomyocytes [9–11]. However, the role of necrosis in the long-term maladaptive cardiac remodeling and in the progression of heart failure after MI was largely ignored since necrosis was believed to be an unregulated, passive form of cell death. Emerging evidence suggests that necrosis may itself be a regulated cellular process. Necroptosis, the best-characterized form of regulated necrotic cell death, exhibits the morphological features of necrosis, but is controlled by defined signaling mechanisms. The receptor-interacting protein kinase 1 (RIP1) and RIP3 are the key signal molecules in regulating and activating of necroptosis. While mixed lineage kinase domain-like (MLKL) has been suggested to act as the executor following the activation of necroptosis [12]. As a new form of programmed cell death, necroptosis has been implicated in a number of pathological conditions such as cancer, neurodegenerative diseases, viral infection and inflammation [13–16]. Recent studies also reported that RIP3-mediated necroptosis is related to the post-ischemic cardiac dysfunction [17,18]. Necrostatin, the inhibitor of the kinase activity of RIP1, could reduce infarct size in response to ischemia-reperfusion (I/R) [19], indicating the pathological role of necroptosis in the post-ischemic injury. However, the role of necroptosis in the sustained loss of cardiomyocytes and underling regulatory mechanism in the context of myocardial infarction remains to be elusive.

In this study, we showed that autophagy flux in the heart tissue was impaired by myocardial ischemic damage *in vivo* and *in vitro*. Importantly, we found that autophagy dysfunction could mediate necroptosis, thereby contribute to the cardiomyocyte loss. Inhibition of necroptosis might be the potential target for preventing post-infarction cardiac remodeling and heart failure.

2. Materials and methods

2.1. Reagents

MTT (3-(4,5-dimethylthiazou-2-yl)-2,5-diphenyltrtrazolium-bromide) and Chloroquine (CQ) were purchased from Sigma-Aldrich (St. Louis, MO, USA). Antibody against LC3(Cat#3868), Beclin-1(Cat#3738), p62(Cat#5114) were from Cell Signaling Technology (Beverly, MA, USA). Antibody against RIP1 (Cat#17519-1-AP) and RIP3 (Cat#17563-1-AP) were from Proteintech (Rosemont, IL, USA). MLKL antibody (Cat#sc-165025) and β-actin antibody (Cat#BS6007M) were from Santa Cruz Biotechnology (California, CA, USA) and Bioworld Technology (St. Louis Park, MN, USA), respectively. Hoechst-33342 and propidium iodide (PI) were form KeyGEN BioTECH, China.

2.2. Animal model and treatment

C57BL/6 mice (22–25 g body weight) were obtained from the experimental animal center of Guangdong Province (Guangzhou, China). Mice received a standard diet and water ad libitum and were treated according to the Guide for the Care and Use of Laboratory Animals, Eighth Edition, (2011, published by The National Academies Press). All experimental procedures were approved by Institutional Animal Care and Use Committee of Guangzhou Medical University.

Myocardial infarction (MI) was induced by permanent ligation of the left anterior descending (LAD) coronary artery. Briefly, mice were anesthetized by sodium pentobarbital (50 mg/kg, ip) and artificially ventilated with an animal ventilator (DH-140, Zhejiang, China). After thoracotomy at the third or fourth intercostal space, the anterior descending branch of left coronary artery was ligated. Mice underwent the same surgical procedure without ligating LAD coronary artery served as sham control. CQ (10 mg/kg/day) was injected intraperitoneally one day after MI and given once a day for 4 weeks.

2.3. Echocardiography

Cardiac function was evaluated by echocardiography with Vevo 2100, a high resolution imaging system (Vevo 2100; VisualSonics Inc., Ontario, Canada) equipped with a 25 MHz imaging transducer. Two-dimensional echocardiographic views of parasternal long-axis and short-axis as well as the apical four chamber were obtained. Cardiac function parameters, including left ventricular internal dimension in diastole (LVIDd), left ventricular internal dimension in systole (LVIDs), the cardiac output (CO), left ventricle ejection fraction (LVEF), left ventricle fractional shortening (LVFS) and other parameters were analyzed according to the instruction of the Vevo 2100.

2.4. Determination of infarct size

The mice were sacrificed and the ventricles were sliced transversely. The slices were incubated with 1% 2,3,5-triphenyl tetrazolium chloride (TTC, pH 7.4) for 20 min at 37 °C. The infarct area was shown as that of TTC-negative.

2.5. Histologic analysis

Mice were sacrificed and the hearts were harvested. After fixed in 4% paraformaldehyde, the tissue blocks were embedded by paraffin and sectioned. Following routine dewaxing, hematoxylin and eosin (H&E) staining and Masson trichrome staining were carried out and the microscopic findings were captured with appropriate objective lenses. Fibrosis in the infarct border zone was quantified using ImageJ software (NIH, version 1.30, http://rsb.info.nih.gov/ij/), and expressed as a percentage of area of fibrotic tissue (blue = collagen) over LV area (above background). More than five fields in three different sections were examined for each mouse by the researcher who was blinded to the treatments.

2.6. Electron microscopy

LV myocardium (1 mm^3) in the border zone of the ischemic heart were pre-fixed in 2.5% glutaraldehyde and 1% osmium tetroxide, followed by incubation with 1% OsO_4 for 3 h at 4 °C, and then dehydrated in graded series of ethanol, and flat embedded in epoxy resin. Ultrathin sections were stained with uranyl acetate and lead citrate, and observed under a transmission electron microscope (HITACHI H-600, Japan).

2.7. Cell culture and treatment

H9C2 cells, a subclone of the original clonal cell line derived from embryonic BD1X rat heart tissue, were purchased from the American Type Culture Collection (ATCC, Rockville, MD), and maintained in Dulbecco's modified Eagles's medium (DMEM, Gibco, USA) supplemented with 10% fetal calf serum, penicillin (100 U/mL) and streptomycin (100 μg/mL). The cells were cultured at 37 °C in a humidified atmosphere with 5% CO_2 and 95% air and passaged by trypsin when confluent. For oxygen-glucose deprivation (OGD), the culture medium of plating cells was changed into DMEM without glucose and serum, and then cultured in an anoxia chamber (InVivo 500, Ruskinn Life Science) saturated with 94%N_2/5%CO_2/1%O_2 for indicated time. CQ (10^{-6} mol/L) was added at 2 h before OGD.

2.8. Cell viability assay

Cell viability was estimated using a colorimetric assay based on tetrazolium dye(MTT(3-(4,5- dimethylthiazou-2-yl)-2,5-diphenyltrtrazolium-bromide) conversion into a blue formazan product. Following OGD, cells were incubated with 10 μL of MTT solution (5 mg/mL). The crystals of formazan precipitate were dissolved using 150 μL of DMSO, and the absorbance was then detected using a Microplate Reader (Bio-Rad Laboratories Inc., Hercules, CA, USA).

2.9. Necrosis analysis

Following OGD, cells were stained with Hoechst-33342 (5 μg/mL) and propidium iodide (PI, 5 μg/mL), and imaged by use of a fluorescence microscope (Olympus 1 × 2-UCB-2). Necrotic cells were identified as having PI-stained nuclei.

2.10. Quantitation of autophagy with mRFP-GFP-LC3 adenovirus

After infected with mRFP-GFP-LC3 adenoviral particles (50 MOI, Hanbio Biotechnology Co., Ltd. Shanghai, China) for 24 h, the cells subjected to OGD for indicated time. Fluorescent signals were captured with the confocal laser scanning microscopy (Nikon America Inc., Melville, NY). The number of autolysosomes and autophagosomes was determined by counting of red puncta or yellow puncta, respectively. Thirty randomly selected cells per experimental group were analyzed.

2.11. Immunostaining of cardiomyocytes

After treatment, the cells were fixed with 4% paraformaldehyde and the cell membrane was labeled with Dil (red) (Invitrogen, Grand Island, NY). The labeled cell was then permeabilized with 0.1% TritonX-100 and blocked with PBS 2% fat-free milk. Immunofluorescent staining was performed using primary antibody against MLKL (1:100) and the second antibody conjugated to Alex-488 (green) (1:1000, Santa Cruz, CA, USA). Nuclei were co-stained with DAPI (blue) (Invitrogen, Grand Island, NY). Cells were observed and imaged by use of confocal laser scanning microscopy (Olympus 1 × 2-UCB-2).

2.12. Generation of RIP3 and Beclin1 construct

shRNA against RIP3 or Beclin1 was constructed into pLKO.1 lentiviral vector (Open Biosystems, Ottawa, Canada) following the manufacturer's instruction. RIP3 and Beclin1 (NM_139342 and BC074011) were amplified from rat cDNA and cloned into pCDH lentivirus vector (Open Biosystems, Ottawa, Canada). All of constructs were verified by DNA sequence analysis.

2.13. Lentiviral preparation and infection in vitro

Lentiviruses were prepared as previously described. Lentiviral plasmid containing no targeted sequences or scramble sequences served as vector control and non-silencing control, respectively. Briefly, lentiviral plasmids carrying cDNAs or shRNAs of RIP3 or Beclin1 were co-transfected with lentiviral packing plasmids into HEK-293 T cells using FuGENE6 reagent (Roche, Indianapolis, IN, USA). High-titer lentiviral stock was produced in HEK-293 T cells 48 h after transfection. Myocytes were infected for 24 h by application of 50 MOI of the lentivirus to the culture medium, and then cultured for a further 72 h prior to treatments and further experimentation. Overexpression or knockdown was confirmed by western blotting.

2.14. In vivo cardiac-specific gene manipulation by intramyocardial injection in mice

In vivo cardiac-specific gene delivery is achieved as described previously [20]. Briefly, under anesthesia, the mouse heart was quickly exposed *via* a left thoracotomy at the fifth intercostal space. Lentivirus carrying RIP3/Beclin1(~2×10^7 PFU) or RIP3/Beclin1 shRNA (~2×10^7 PFU) was delivered *via* three separate intramyocardial injections into the left ventricular free wall. Myocardial target gene expression was analyzed 4 days after virus injection by western blotting.

2.15. Western blotting analysis

After treatment, the proteins extracted from heart tissues or cardiomyocytes were separated by SDS-PAGE and transferred to PVDF membranes (Roche Molecular Biochemicals, Mannheim, Germany). The membranes were blocked and detected with anti-LC3 antibody (1:1000), anti-Beclin1 antibody (1:1000), anti-p62 antibody (1:1000), anti-RIP3 antibody (1:1000), anti-RIP1 antibody (1:1000) or anti-β-actin antibody (1:4000), respectively. The density of target bands was accurately determined by the computer-aided Quantity One analysis system. In order to avoid variability from different treatment time, mice or the proteins for detection *per se*, the expression of proteins in the infarct boarder zone in MI mice was normalized to that of the sham mice in each time point, and β-actin served as a loading control.

2.16. Statistical analysis

All values were expressed as mean ± standard deviation. Differences between two groups were analyzed by Student *t* test, while differences among two more groups were evaluated by one-way ANOVA for independent samples or by ANOVA for repeated measurements followed by Tukey post-hoc test using software of SPSS 11.5 (SPSS Science, Chicago, IL, USA). A value of $P < 0.05$ was taken as statistically significant.

3. Results

3.1. Cardiac dysfunction and heart failure were induced by myocardial infarction in mice

A permanent ligation of the left anterior descending (LAD) coronary artery was used to induce myocardial infarction in mice. The heart-to-body weight ratio (HW/BW) of mice was calculated and the myocardial infarction area was detected by TTC staining. As shown in Fig. 1A and B, both the HW/BW and the myocardial infarction area were increased over time after MI as compared to sham mice. Following MI, the hearts in MI mice exhibited growing thinned left ventricular anterior wall (LVAW) and left ventricular posterior wall (LVPW), but enlarged LV dimension (LVID) either at the end of diastole or at the end of systole. The fractional shortening (FS) and ejection fraction (EF) of left ventricular in MI mice were also significantly decreased from 1 week after MI, indicating persistent impaired systolic function in MI mice from 1 week. The transmitral filling pattern obtained by echocardiography showed there was no significant difference concerning the ratio of E-wave velocity to A-wave velocity (E/A) between MI mice and sham mice from 1 to 4 weeks. However, isovolumetric relaxation time (LVRT) and isovolumetric constriction time (LVCT) were prolonged in MI mice from 2 weeks, and the early diastolic mitral annulus velocity/late diastolic mitral annulus velocity (e'/a') was significantly reduced from 4 week, implying the gradually impaired diastolic function in MI mice from 2 weeks and remarkable diastolic dysfunction in MI mice from 8 weeks as reflecting by significant increase of the ratio of E/A. By week eight after MI, the ejection time (ET) was markedly prolonged with the cardiac output (Co) concomitantly decreased in MI mice than that of sham mice (Fig. 1C and D), indicating that MI mice progressed to the heart failure with both of systolic and diastolic dysfunction.

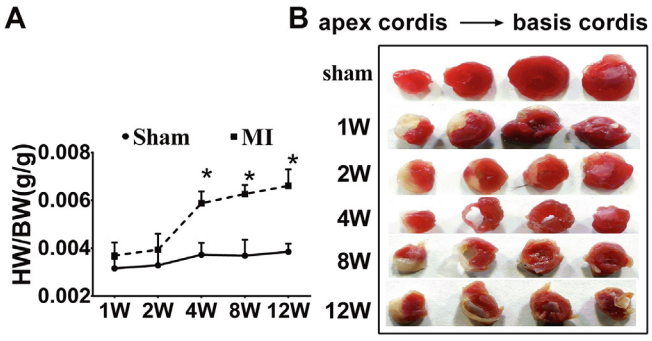

Fig. 1. Cardiac dysfunction induced by myocardial infarction (MI). Myocardial infarction was induced by permanent ligation of the left anterior descending (LAD) coronary artery of mice. (A) The ratio of heart weight to body weight (HW/BW) was analyzed at indicated time point after ligation surgery in each experimental group (Student *t* test, $n = 6$, $^{*}P < 0.05$ *vs.* sham). (B) Representative images of heart sections with TTC staining of the infarcted area. (C) Representative M-mode echocardiograms and the analyzed results of cardiac function obtained from mice in each experimental group (ANOVA for repeated measurements, $n = 6$, $^{*}P < 0.05$ or $^{**}P < 0.01$ *vs.* sham). (D) Representative transmitral flow and tissue Doppler echocardiograms and the analyzed results of cardiac function obtained from mice in each experimental group (ANOVA for repeated measurements, $n = 6$, $^{*}P < 0.05$ or $^{**}P < 0.01$ *vs.* sham).

shown in Fig. 2A, myocardial infarction induced the significant upregulation of beclin1 in the border zone of infarcted heart from 1 day, and remained higher until 12 weeks as compared to the sham mice. The value of LC3 II/I was also increased from 1 day to 3 days, but decreased quickly from 1 week after MI. On the contrary, the expression of p62 was reduced at 1 day after MI, but increased persistently until 12 weeks. These results indicated that autophagy activity was induced by MI at the very early stage, but autophagy flux (the entire process of autophagy) was hampered with the progression of cardiac dysfunction.

The autophagic activity in H9C2 cardiomyocytes subjected to OGD *in vitro* was also examined. The results showed that OGD treatment time-dependently upregulated expression of beclin1 and LC3II/I (Fig. 2B). The expression of p62 was downregulated within 3 h after OGD but showed a marked accumulation after 6 h. As the increase in LC3II/I and accumulation of p62 could be from either increased induction of autophagy or, on the contrary, due to inefficient autophagic degradation of the cargo, we subsequently examined the effects of chloroquine (CQ), a lysosomal inhibitor, on the expression of LC3 and p62/SQSTM1 induced by OGD. Notably, pretreatment cells with chloroquine (CQ) increased the level of either LC3 II/I or p62 to a level comparable to that without CQ treatment, and did not further increase the expression of LC3 II/ I or p62 from 6 h after OGD (Fig. 2B), indicating that autophagy was induced by OGD in a short time, then followed by the defective autophagic degradation. Impaired autophagy

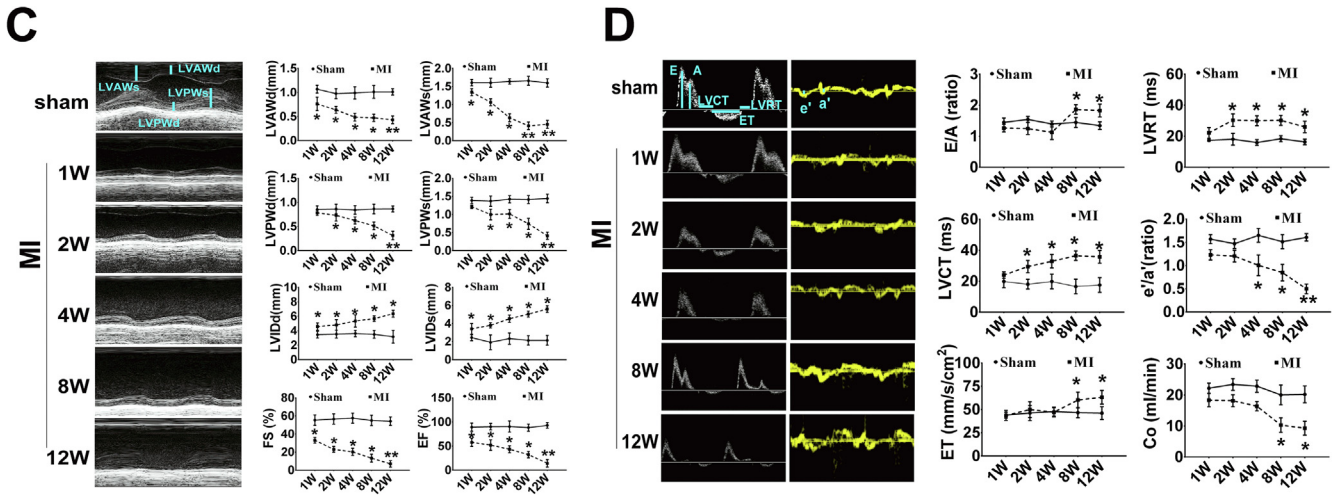

Fig. 1. (*continued*)

3.2. Autophagy flux was impaired by myocardial ischemia in vivo and in vitro

Autophagy is a highly dynamic, multi-step process, typically including the initiation of autophagy to form phagophore, phagophore expands into an autophagosome, then followed by fusion with lysosomes to form the autolysosomes and final degradation of the contents. Beclin1, a mammalian homology of yeast Atg6/Vps30, is an initiator of autophagy and required for autophagosome formation. Microtubule-associated protein 1 light chain 3 (LC3) is the most widely monitored autophagy-related protein which participated in the autophagosome formation by conjugating cytosolic LC3I with PE to produce lipidated autophagosome-associated LC3II, therefore, the ratio of LC3II/I reflects the accumulation of autophagosomal vesicles. P62/SQSTM1 is an ubiquitin binding adaptor protein, which bound to polyubiquitinated proteins incorporated into the completed autophagosome and are degraded in autolysosomes, thus serving as an index of autophagic degradation. To determine the autophagic activity during the progression of heart failure induced by MI, we monitored the dynamic changes of beclin1, LC3 and p62/SQSTM1 in infarct myocardium after MI. As flux induced by OGD in cardiomyocytes was also confirmed by use of tandem RFP-GFP-LC3 fluorescence analysis (Fig. 2C). OGD treatment time-dependently increased the numbers of yellow puncta (autophagosomes). The number of red puncta (autolysosomes) was increased within 3 h after OGD, but followed by a decreases 12 h after OGD.

3.3. Impairment of autophagy flux contributed to cardiomyocyte death and the adverse cardiac remodeling

The contribution of impaired autophagy to OGD-induced cardiomyocyte death was assessed by utilizing CQ or lentiviral overexpression or knockdown of beclin1. As shown in Fig. 3A, targeted shRNA against beclin1 achieved significant knockdown of beclin1 protein. While, beclin1 lentiviruses increased the expression of beclin1 protein to 183.6% than that of control. Neither scramble sequence nor empty lentiviral plasmid affected the expression of beclin1. Beclin1 overexpression increased, while beclin1 knockdown significantly decreased the level of LC3 II/I, the number of the autophagosome and autophagolysosome. Different from beclin1 shRNA, CQ treatment markedly decreased the number of autophagolysosome, but caused the remarkable

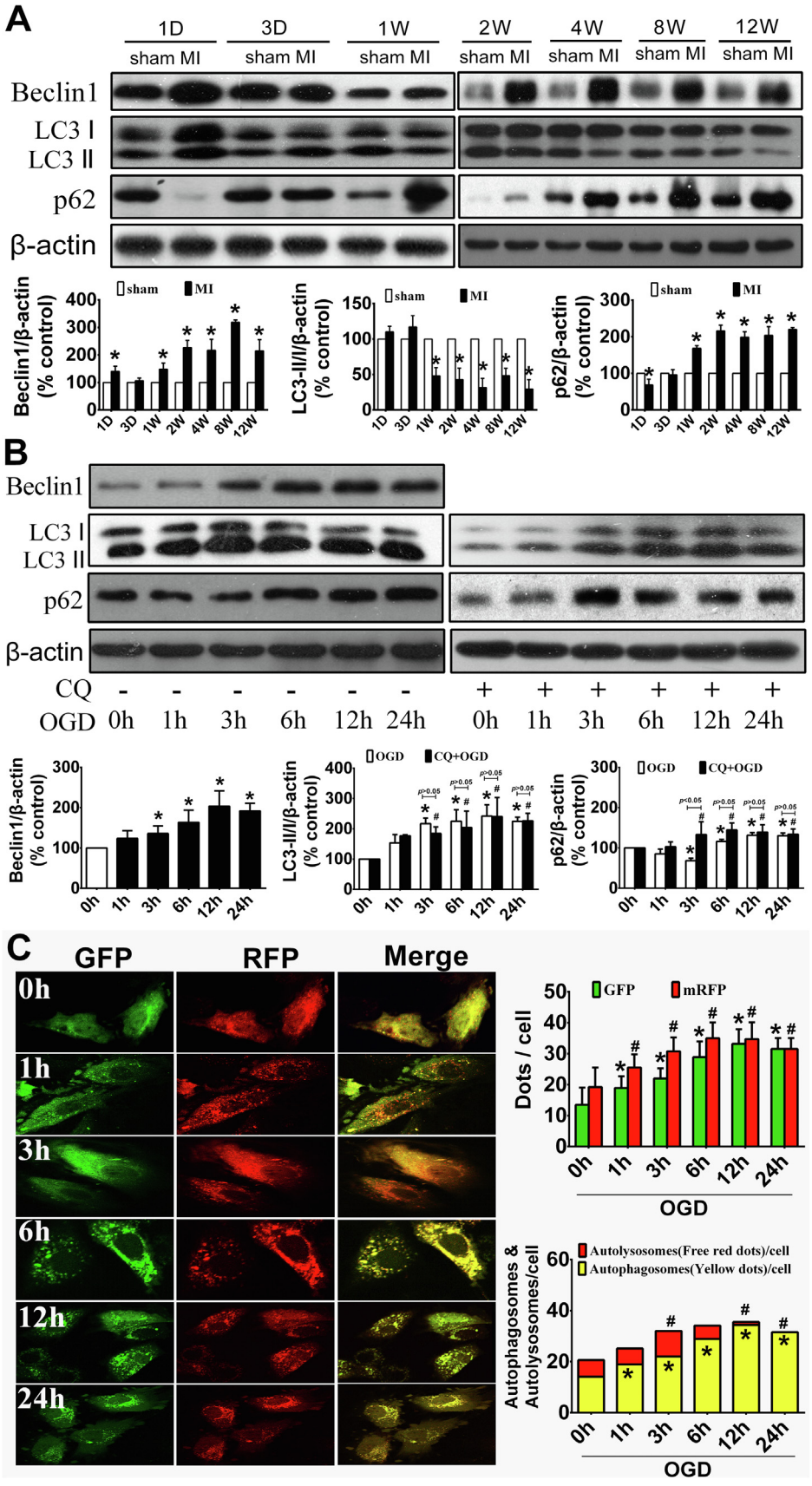

Fig. 2. Autophagy flux was impaired by myocardial ischemia *in vivo* and by OGD *in vitro*. (A) Autophagic markers in the border zone of infarct myocardium were determined by western blotting at indicated time point after MI (Student *t* test, $n = 3$, $^{*}P < 0.05$ *vs.* sham. The expression of proteins in MI mice was normalized to that of the sham mice in each time point, and β-actin served as a loading control). (B) After pretreated with or without CQ for 2 h, H9C2 cells were subjected to OGD and the expression of beclin1, LC3 and p62 was examined by western blotting at indicated time point (one-way ANOVA, $n = 5$–6, $^{*}P < 0.05$ *vs.* 0 h in OGD, $\#P < 0.05$ *vs.* 0 h in CQ + OGD). (C) After infected with mRFP-GFP-LC3 adenoviral particles for 24 h, the cells were subjected to OGD. Fluorescent signals were captured with the confocal laser scanning microscopy at indicated time point and the number of autolysosomes and autophagosomes was determined by counting of red puncta or yellow puncta, respectively (one-way ANOVA, $^{*}P < 0.05$ or $\#P < 0.05$ *vs.* 0 h in yellow puncta or red puncta, respectively. Thirty randomly selected cells per experimental group were analyzed). (For interpretation of the references to colour in this figure legend, the reader is referred to the web version of this article.)

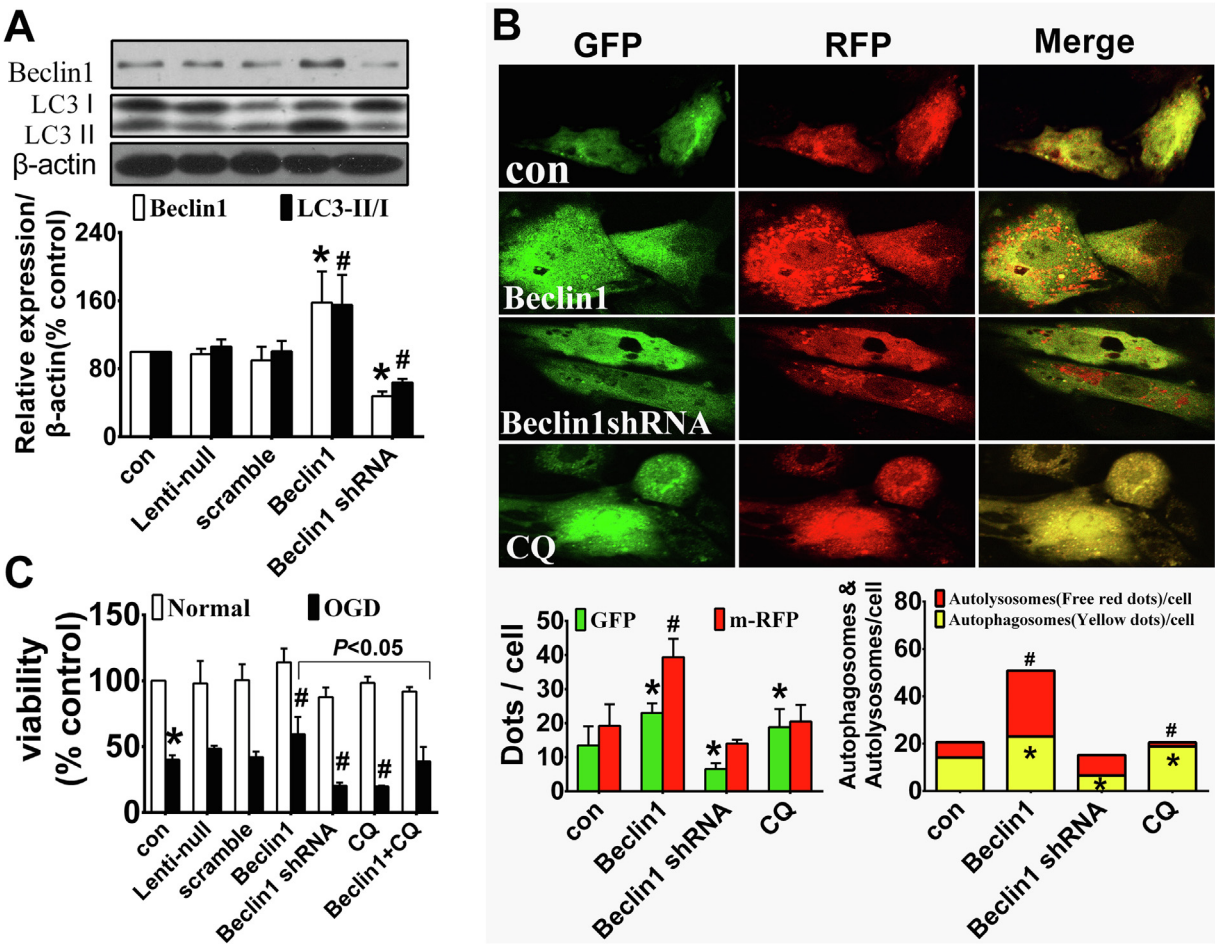

Fig. 3. Impaired autophagy flux contributed to cardiomyocyte death. H9C2 cells infected with lentivirus expressing beclin1 or beclin1 shRNA were subjected to OGD for 24 h. (A) The expression of beclin1 and LC3 were examined by western blotting (one-way ANOVA, $n = 3$–5, $^*P < 0.05$ *vs.* control in Beclin1, $\#P < 0.05$ *vs.* control in LC3). (B) Autolysosomes and autophagosomes were determined by use of a tandem mRFP-GFP-LC3 adenovirus in H9C2 cell. The red puncta indicated autolysosomes and the yellow puncta indicated autophagosomes, respectively (one-way ANOVA, $^*P < 0.05$ or $\#P < 0.05$ *vs.* control in yellow puncta or red puncta, respectively. Thirty randomly selected cells per experimental group were analyzed). (C) The cell viability was assessed by MTT assay (one-way ANOVA, $n = 8$, $^*P < 0.05$ *vs.* normal control, $\#P < 0.05$ *vs.* OGD). (For interpretation of the references to colour in this figure legend, the reader is referred to the web version of this article.)

accumulation of the autophagosome (Fig. 3A and B). Treatment of cells with OGD for 24 h decreased the cell viability to 32.8%. Cardiomyocyte death was aggravated either by CQ or by beclin1 knockdown, but was rescued by beclin1 overexpression. Notably, pretreatment of cells with CQ, the inhibitory effect of beclin1 overexpression on the OGD-induced necrotic cell death was blunted (Fig. 3C).

The involvement of impaired autophagy flux in cardiac remodeling and dysfunction after MI was further investigated by treatment of MI mice with CQ (10 mg/kg/day) from 1 day after LAD ligation for 4 weeks, or by performing cardiac-specific gene overexpression or knockdown of beclin1 through *in vivo* intramyocardial delivery of lentivirus-encoded beclin1 or beclin1 shRNA 3 days before MI. Intramyocardial infection of lentiviral beclin1 or lentiviral beclin1 shRNA led to significant increase or decrease in beclin1 expression in the cardiac *peri*-infarct zones than that of sham mice (Fig. 4A), respectively. Compared with MI mice, both of beclin1 deletion and CQ treatment significantly reduced the LVEF, LVFS and LVAW, but increased LV dimension as early as 2 weeks after MI. The deteriorated diastolic function in beclin1 deletion mice and CQ-treated mice was also more serious than that of MI mice as evidenced by remarkably prolonged LVRT, LVCT and increased ratio of E/A but, decreased ratio of e'/a'. The substantial decrease in cardiac output in beclin1 deletion mice and CQ-treated mice was associated with accelerated progression of heart failure in comparison to MI mice (Fig. 4B and C). Electron microscopic analysis of the sham mice heart showed that the presence of cytoplasmic vacuoles that resembled autophagosomes in the border zone (Fig. 4D). However, less autophagosomes were found in MI mice heart and beclin1 deletion mice heart, while more autophagosomes accumulation was found in the heart of CQ-treated mice. Masson-Trichrome staining revealed that the MI scar size, deranged myocardial fibers and cardiac fibrosis were significantly aggravated either by beclin1 deletion or by CQ treatment as compared to MI mice (Fig. 4E and F), indicating that CQ treatment and cardiac beclin1 deletion aggravated autophagy dysfunction and long-term adverse post-infarct remodeling. On the contrary, cardiac-specific overexpression of beclin1 significantly increased the autophagic vacuoles and ameliorated the post-infarct systolic dysfunction by increasing LVFS, and the thickness of left ventricular wall, and by decreasing the LVID 2 weeks after MI. However, neither improved systolic dysfunction was sustained with time nor the post-infarct diastolic dysfunction got better by cardiac-specific overexpression of beclin1 although the ratio of e'/a' was increased at 4th week after MI. Microscopic analyses of the beclin1 mice heart showed that the deranged myocardial fibers and loss of continuity of the myofilaments after MI were lessoned than that of MI mice, but more fibrosis was found between myocardial fibers in the infarcted-heart border of beclin1 mice, indicating that constitutive upregulation

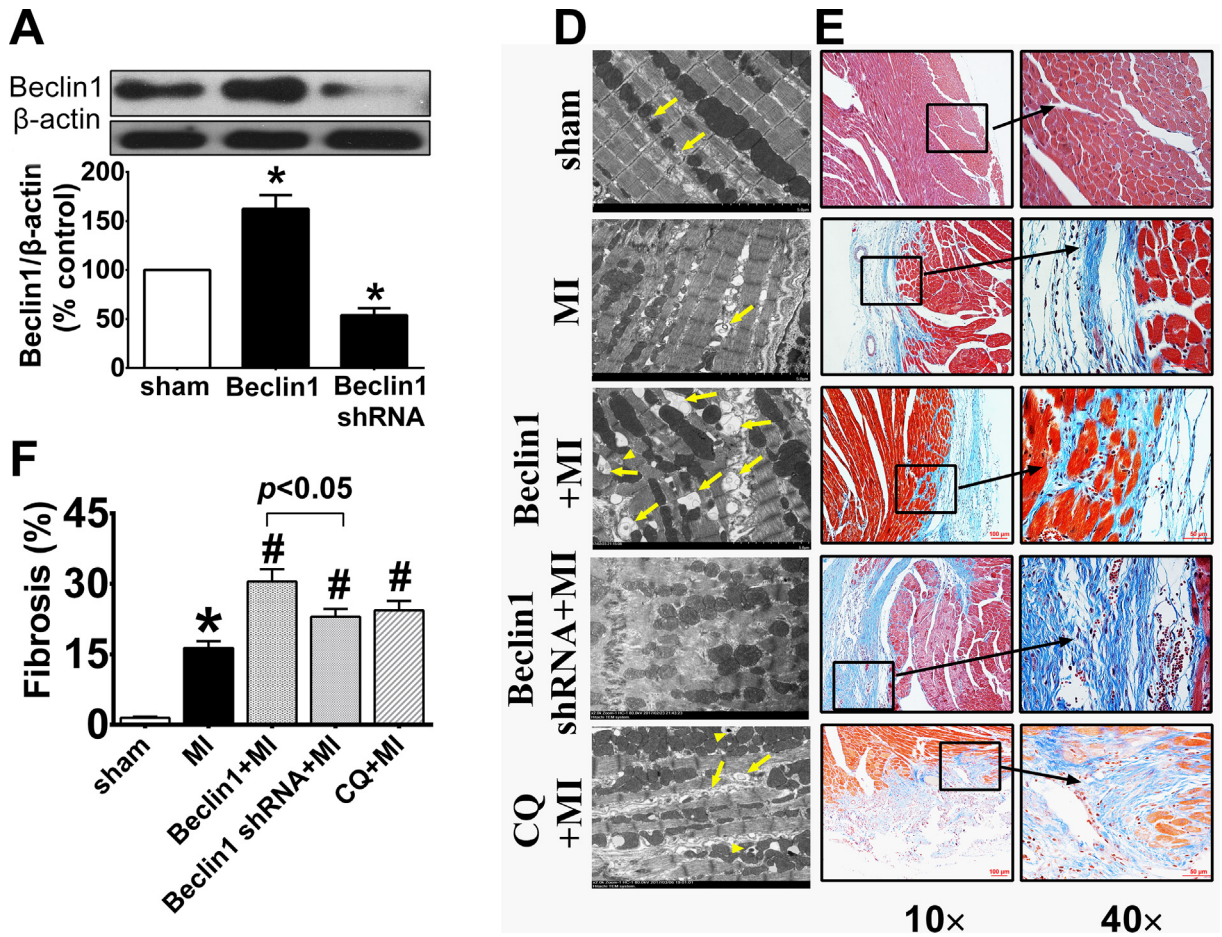

Fig. 4. Impaired autophagy flux contributed to the adverse cardiac remodeling. Autophagy was perturbed by intraperitoneal injection of CQ (10 mg/kg/day) one day after MI for 4 weeks or by cardiac-specific delivery of lentiviral beclin1 or lentiviral beclin1 shRNA 3 days before MI. (A) Western blotting showing the successful knocking down or overexpression of beclin1 in the border zone of infarct heart (one-way ANOVA, $n = 4$, $^*P < 0.05$ *vs.* sham). (B) Representative M-mode echocardiograms and the analyzed results of cardiac function obtained from mice in each experimental group (ANOVA for repeated measurements, $n = 6$, $^*P < 0.05$ *vs.* MI at the same time point). (C) Representative transmitral flow and tissue Doppler echocardiograms and the analyzed results of cardiac function obtained from mice in each experimental group (ANOVA for repeated measurements, $n = 6$, $^*P < 0.05$ *vs.* MI at the same time point). (D) Ultrastructure analysis of the infarct heart showing the autophagosomes (multimembrane vacuoles, arrow heads) and autolysosomes (electron dense structures, arrows) in the border myocardium 4 weeks after MI. (E) Representative cross-sectional images showing interstitial fibrosis with Masson staining. (F) Analysis results for Masson staining (one-way ANOVA, $n = 6$, $^*P < 0.05$ *vs.* sham, $\#P < 0.05$ *vs.* MI).

of autophagy in the heart might be involved in the heart fibrosis.

3.4. Necroptosis was persistently activated in response to ischemia in vivo and in vitro

To probe a potential pathological role of necroptosis in cardiac remodeling after MI, the expression of necroptosis-related proteins RIP1 and RIP3 were quantified by western blot analysis. The results showed that the protein levels of RIP1 and RIP3 in the border zone of infarcted heart were upregulated significantly from 1 to 12 week after MI as compared to the sham mice (Fig. 5A), indicating that necroptosis was induced with the progression of heart failure. Consistent with activation of necroptosis in response to myocardial infarction, the Oxygen and Glucose deprivation (OGD) treatment time-dependently increased the H9C2 cell death and the number of PI-positive necrotic cardiomyocytes (Fig. 5B and C). Treatment of cells with OGD for 12 h to 24 h caused the marked increases of the expression of RIP1 and RIP3 in cardiomyocytes (Fig. 5D), and induced the MLKL, a downstream effector of necroptosis, translocated from cytoplasm to membrane (Fig. 5E).

3.5. Impairment of autophagy flux contributed to cardiomyocyte death by activation of necroptosis

As shown in Fig. 6A–C, the expression of RIP3 in the border zone of the infarct heart or in the OGD-treated H9C2 cells was upregulated significantly either by beclin1 knockdown or by CQ treatment, but downregulated by beclin1 overexpression. Both of CQ pretreatment and beclin1 knockdown markedly increased OGD-induced necrotic cell death. By contrast, the OGD-induced necrotic cell death was significantly ameliorated by beclin1 overexpression (Fig. 6D). Notably, after knocking down of RIP3 in H9C2 cells, the promoted effects of CQ on the OGD-induced necrotic cell death was abolished (Fig. 6E).

3.6. Necroptosis mediated the loss of cardiomyocytes and the cardiac dysfunction after myocardial infarction

The involvement of necroptosis in OGD-induced cardiomyocyte death was examined by utilizing lentiviral overexpression or knockdown of RIP3. As shown in Fig. 7A, infecting cells with lentiviruses expressing RIP3 or RIP3 shRNA achieved significant overexpression or knockdown of RIP3 protein, respectively. Neither scramble sequence nor empty lentiviral plasmid affected the expression of RIP3. Knocking

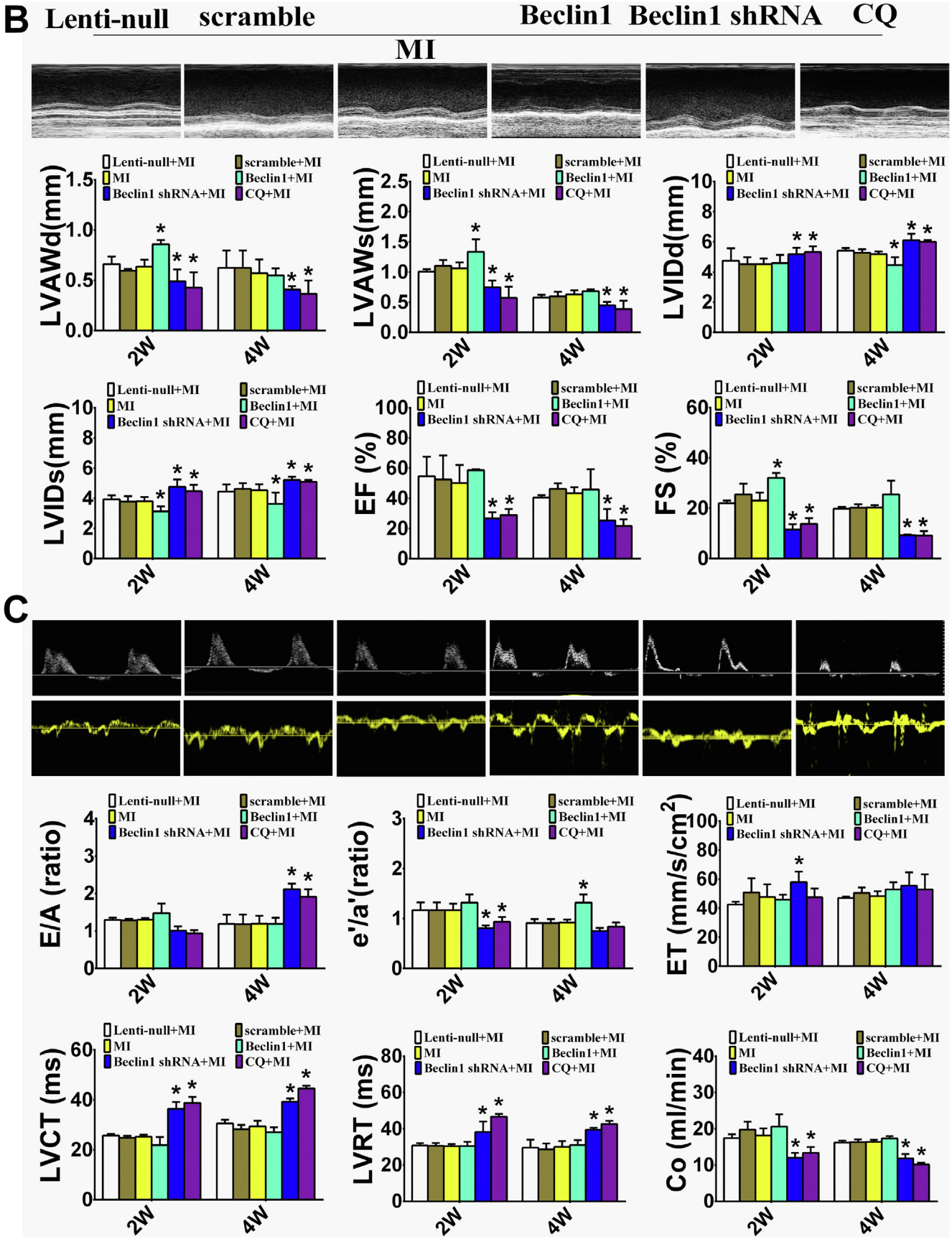

Fig. 4. (*continued*)

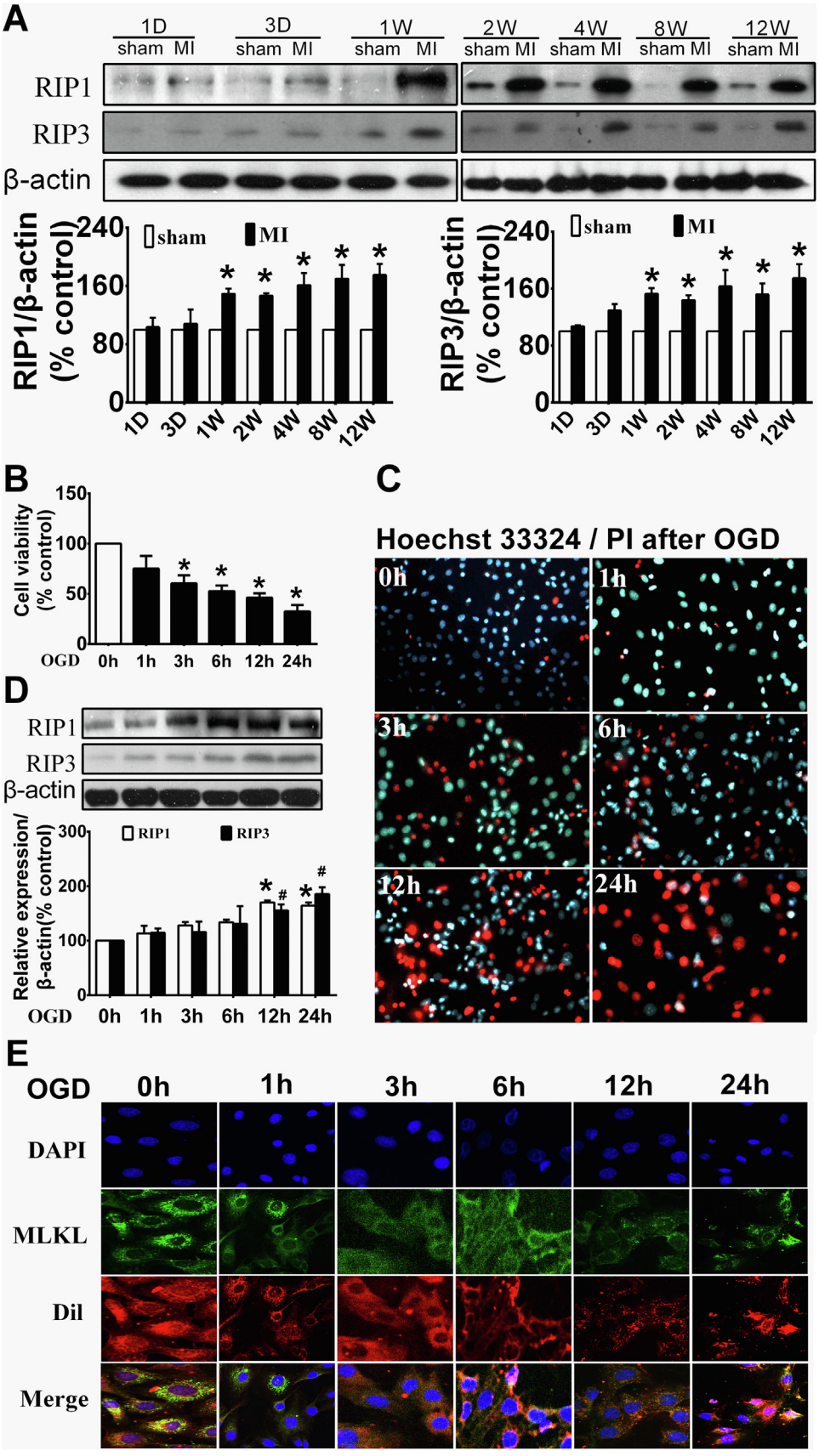

Fig. 5. Necroptosis was persistently activated in response to ischemia *in vivo* and by OGD *in vitro*. (A) Myocardial infarction was induced by permanent ligation of LAD in mice and the expression of indicated necroptosis-related protein in the border zone of infarct heart was determined by western blotting at indicated time point after ligation surgery in sham and MI mice (Student *t* test, $n = 6$, $^{*}P < 0.05$ *vs.* sham. The expression of proteins in MI mice was normalized to that of the sham mice in each time point, and β-actin served as a loading control). H9C2 cells were subjected to the OGD for indicated time point. (B) The cell viability was assessed by MTT assay (one-way ANOVA, $n = 8$, $^{*}P < 0.05$ *vs.* 0 h). (C) Cell necrosis was evaluated by Hoechst/PI staining. (D) The expression of RIP1 and RIP3 were determined by western blotting (one-way ANOVA, $n = 4$–8, $^{*}P < 0.05$ *vs.* 0 h in RIP1, $^{\#}P < 0.05$ *vs.* 0 h in RIP3). (E) Immunofluorescent staining showing the translocation of MLKL from cytoplasm to membrane.

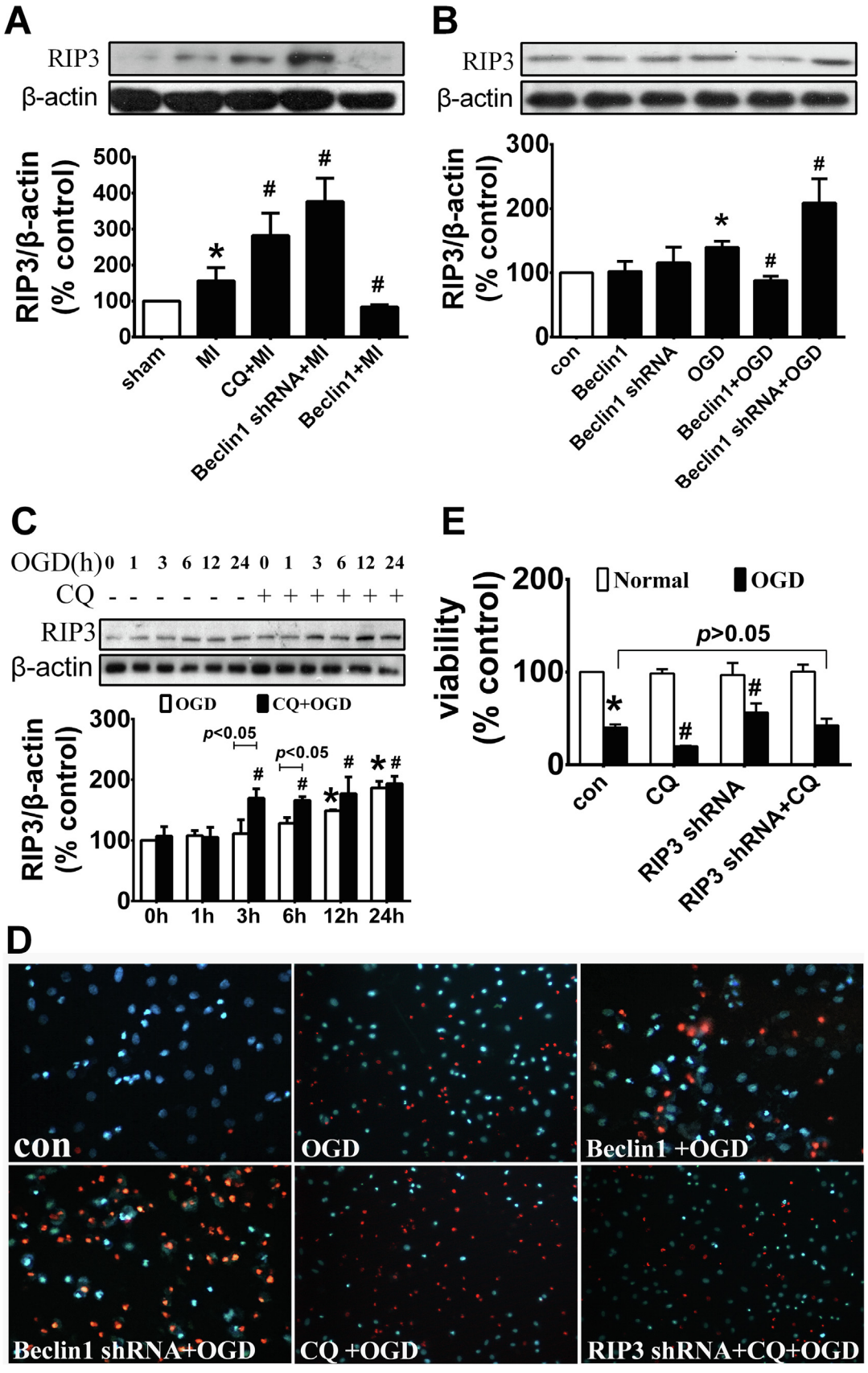

(caption on next page)

Fig. 6. Impaired autophagy flux contributed to cardiomyocyte death by activating of necroptosis. (A) Autophagy was perturbed by intraperitoneal injection of CQ (10 mg/kg/day) one day after MI for 4 weeks or by cardiac-specific delivery of lentiviral beclin1 or lentiviral beclin1 shRNA 3 days before MI. Western blotting showing the expression of RIP3 in the border zone of infarct heart (one-way ANOVA, $n = 4$–6, $^*P < 0.05$ *vs.* sham). (B) H9C2 cells infected with lentivirus expressing beclin1 or beclin1 shRNA were subjected to OGD for 24 h. The expression of RIP3 was examined by western blotting (one-way ANOVA, $n = 6$, $^*P < 0.05$ *vs.* control, $\#P < 0.05$ *vs.* OGD). (C) H9C2 cells were subjected to OGD for indicated time point in the presence or absence of CQ. The expression of RIP3 was examined by western blotting (one-way ANOVA, $n = 4$, $^*P < 0.05$ *vs.* 0 h in OGD, $\#P < 0.05$ *vs.* 0 h in CQ + OGD). (D) H9C2 cells infected with lentivirus expressing beclin1, beclin1 shRNA or RIP3 shRNA were subjected to OGD for 24 h in the presence or absence of CQ. Cell necrosis was evaluated by Hoechst/PI staining. (E) After knocking down of RIP3 with lentiviral RIP3 shRNA, the H9C2 cells were subjected to OGD for 24 h in the presence or absence of CQ. The cell viability was assessed by MTT assay (one-way ANOVA, $n = 6$, $^*P < 0.05$ *vs.* normal control, $\#P < 0.05$ *vs.* OGD).

down of RIP3 significantly decreased the number of PI-positive necrotic cardiomyocytes and increased the cell survival of OGD-treated cardiomyocyte. In contrast, cardiomyocyte death induced by OGD was aggravated by RIP3 overexpression (Fig. 7B and C).

To further investigate the involvement of necroptosis in cardiac dysfunction induced by MI, we performed cardiac-specific gene overexpression or knockdown of RIP3 by *in vivo* intramyocardial infection of lentivirus-encoded RIP3 or lentivirus-encoded RIP3 shRNA 3 days before MI. Intramyocardial delivery of lentiviral RIP3 or lentiviral RIP3 shRNA led to remarkable increase or decrease in RIP3 expression in the cardiac *peri*-infarct zones than that of sham mice (Fig. 8A), respectively. Compared with MI mice, the heart of RIP3 mice exhibited the aggravated systolic and diastolic dysfunction as marked by reduction of LVEF, LVFS and the thickness of left ventricular wall, but enlarged LV dimension, as well as prolonged LVRT, LVCT and increased the ratio of E/A. The cardiac output in RIP3 mice was also significantly decreased 8 weeks after MI, indicating accelerated progression of heart failure in comparison to MI mice (Fig. 8B and C). Consistently, the heart of RIP3 mice showed the significantly increased infarct size and collagen formation by TTC and Masson's trichrome staining as compared to MI mice (Fig. 8D). Furthermore, the results from histological analysis and electron microscopic evaluation revealed the heart of RIP3 mice showed more deranged myocardial fibers, loss of continuity of the myofilaments, increased cardiac fibrosis and mitochondrial damage than MI mice. By contrast, both the cardiac systolic and diastolic function in mice with RIP3 knockdown was much better than that of MI mice. Also, myocardial fibrosis, infarct size and myocardial injury were dramatically alleviated as compared to the MI mice (Fig. 8E–G), indicating that suppression of necroptosis improved long-term adverse post-infarct remodeling.

4. Discussion

Left ventricular adverse remodeling in response to myocardial damage is a powerful indicator for heart failure and cardiovascular death after myocardial infarction. Herein we reported that mice subjected to MI by means of coronary artery ligation successfully developed the progressive left ventricle remodeling and ultimately heart failure as manifested by structural thinning and dilation of left ventricular with a progressive and sharp decline in systolic and diastolic function. In response to myocardial ischemic damage, autophagy activity in the mice heart was upregulated quickly but followed by the process of impaired

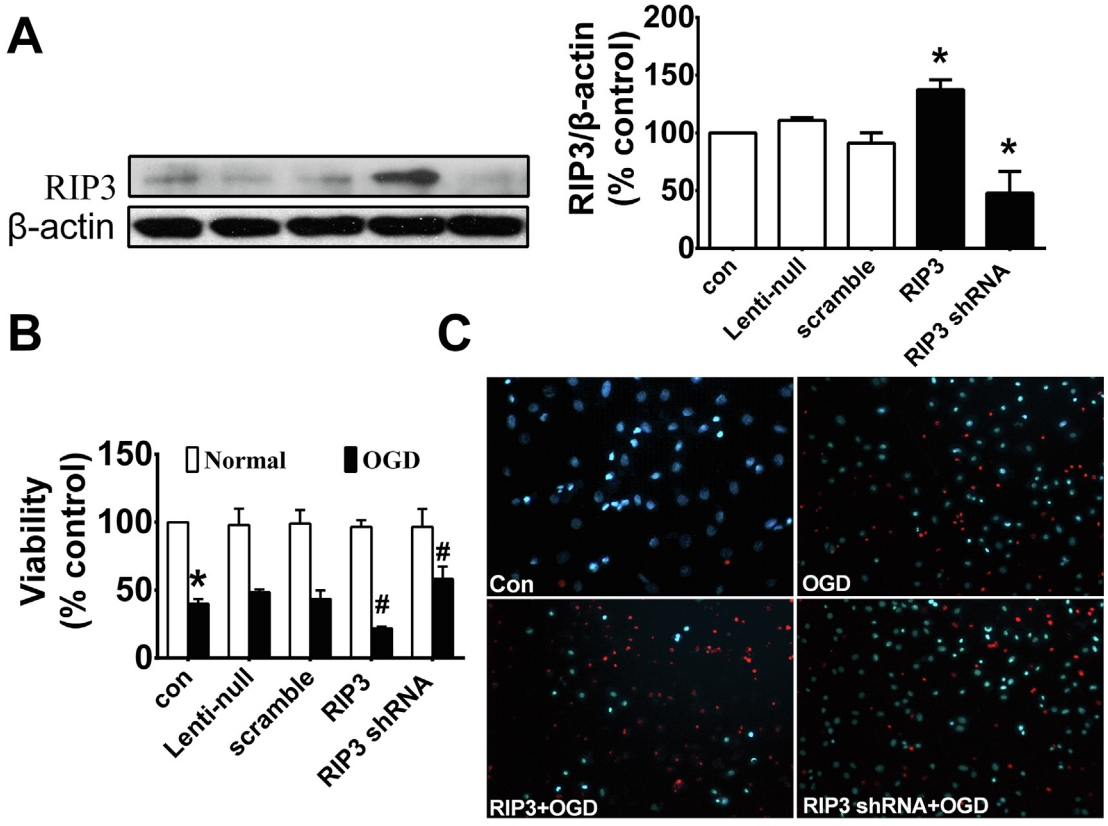

Fig. 7. Necroptosis mediated the loss of cardiomyocytes. (A) The level of RIP3 was successfully downregulated or upregulated in H9C2 cells by infecting lentiviral RIP3 shRNA or lentiviral RIP3, respectively. Lentiviral plasmid containing no targeted sequences or scramble sequences served as vector control and non-silencing control (one-way ANOVA, $n = 4$, $^*P < 0.05$ *vs.* control). After knockdown or overexpression of RIP3, H9C2 cells were subjected to the OGD for 24 h. (B) The cell viability was assessed by MTT assay (one-way ANOVA, $n = 6$, $^*P < 0.05$ *vs.* control, $\#P < 0.05$ *vs.* OGD). (C) Cell necrosis was evaluated by Hoechst/PI staining.

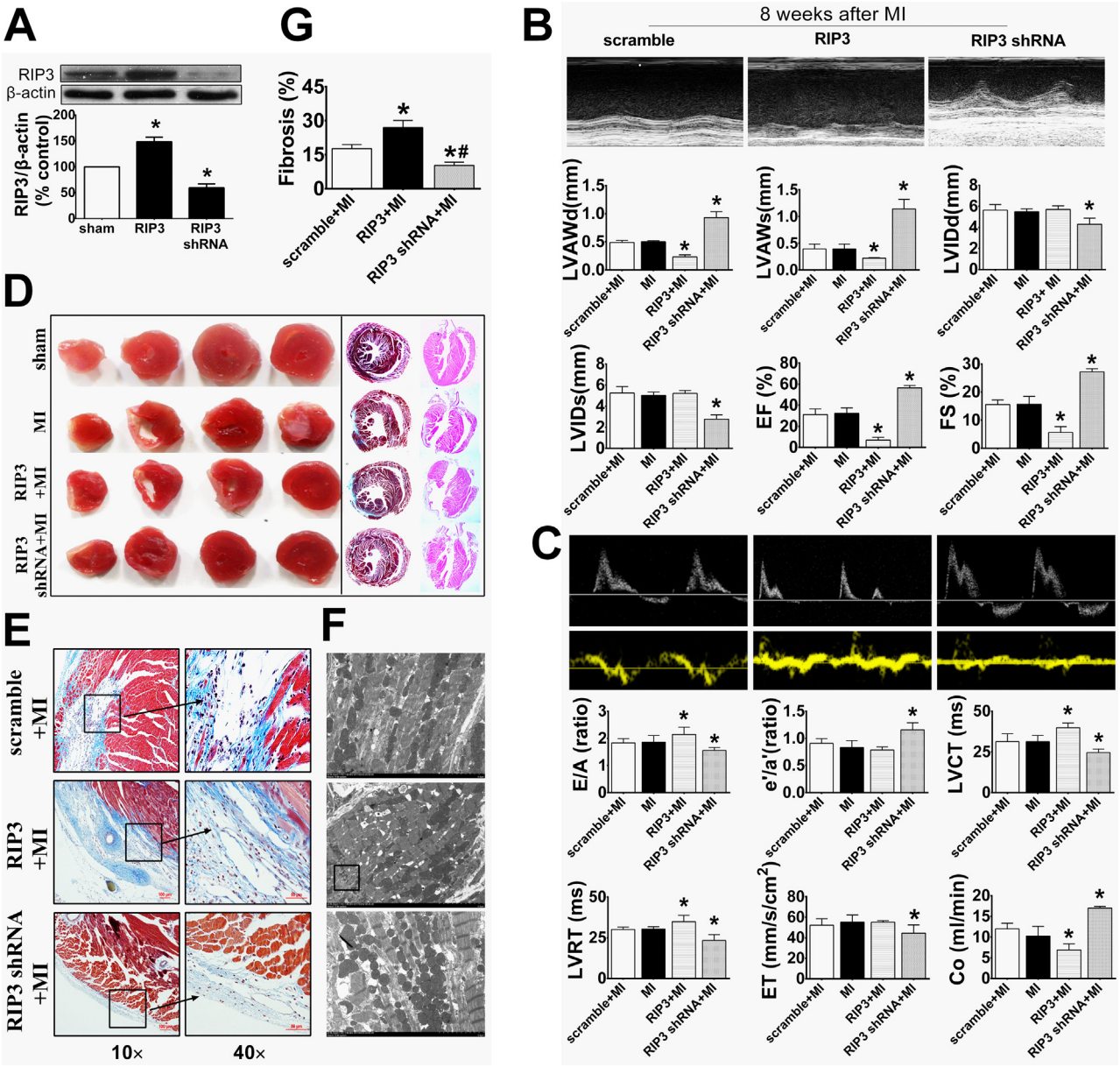

Fig. 8. Necroptosis mediated the cardiac dysfunction and adverse cardiac remodeling after MI. (A) Western blotting showing the successful knocking down or overexpression of RIP3 in the border zone of infarct heart by cardiac-specific delivery of lentiviral RIP3 or lentiviral RIP3 shRNA (one-way ANOVA, $n = 4$, $^*P < 0.05$ *vs.* sham). (B) Representative M-mode echocardiograms and the analyzed results of cardiac function obtained from mice in each experimental group (one-way ANOVA, $n = 6$, $^*P < 0.05$ *vs.* MI). (C) Representative transmitral flow and tissue Doppler echocardiograms and the analyzed results of cardiac function obtained from mice in each experimental group (one-way ANOVA, $n = 6$, $^*P < 0.05$ *vs.* MI). (D) Representative cross-sectional images showed the infarcted area with TTC staining and Masson staining. (E) Representative cross-sectional images showed the interstitial fibrosis with Masson staining. (F) Ultrastructure analysis of the infarct heart 8 weeks after MI (square frame showing damaged mitochondrial). (G) Analysis results for Masson staining (one-way ANOVA, $n = 6$, $^*P < 0.05$ *vs.* scramble + MI, $\#P < 0.05$ *vs.* RIP3 + MI).

autophagy flux with the progressive cardiac dysfunction. More important, the impairment of autophagy flux induced by myocardial ischemia could mediate necroptosis and thereby contribute to the cardiomyocyte loss and post-infarct cardiac remodeling. Constitutive activation of necroptosis by forced cardiac-specific overexpression of RIP3 aggravated necrotic cardiomyocyte death and post-infarct cardiac remodeling and cardiac dysfunction, but all of which could be ameliorated by inhibition of necroptosis by RIP3 deletion, suggesting that autophagy dysfunction-mediated necroptosis mechanistically contributed to adverse ventricular remodeling and promoted heart failure after myocardial Infarction.

Accumulating evidence indicates that autophagy plays a critical role in determining the cell fate. As a fundamental cellular mechanism for cell survival, appropriate autophagy is essential for the maintenance of cardiac homeostasis under physiological conditions or in response to stress. However, dysregulated autophagy has been reported in the adverse cardiac remodeling and heart failure [21]. Multiple studies have demonstrated that cardiomyocyte autophagy is quickly increased in response to ischemic stress at the acute phase after MI. To date, however, it is the subject of debate that increased cardiomyocyte autophagy at the acute ischemic phase was followed by constitutive upregulation of autophagy or by impaired autophagy flux during the latter chronic stage. Therefore, some data supported that upregulation of autophagy was associated with a cardioprotective effect on the adverse cardiac remodeling, but others showed that up-regulation of autophagy was detrimental and exacerbated long-term cardiomyocyte ischemic injury

[5,22–24]. In this study, we demonstrated that autophagic process in the infarct border myocardium, including initiation of autophagy, autophagosome formation and autophagosome degradation, was accelerated within 1 day in response to ischemia, as shown by increased level of beclin1 and the value of LC3 II/I, but decreased level of p62. However, the increased autophagy at acute stage after MI was followed by the defective autophagy flux as evidenced by decreased LC3 II/I and increased accumulation of p62, while the level of beclin1 remained higher until 12 weeks. Our data on cardiomyocytes led to the same conclusion that upregulated autophagy induced by the "starved" state of OGD was followed by impaired autophagy flux. Especially, this kind of impaired autophagy flux was further supported by use of the lysosomal inhibitor CQ and GFP-RFP-LC3 adenovirus. These findings supported that the early accelerated autophagy flux probably was an adaptive stress reaction for the acute ischemia to prevent myocardium from acute ischemic injury and promoted the survival of cardiomyocytes. However, the following impaired autophagy, possible due to insufficient ATP or energy exhausted after ischemia, might be involved in the long-term cardiac dysfunction and adverse remodeling after MI. Indeed, our results on CQ and cardiac-specific beclin1 knockdown showed that impairment of autophagy flux aggravated ventricular remodeling and cardiac dysfunction in mice subjected to MI. Consistent with several previous reports in which activation of autophagy in MI mice by rapamycin for 2 to 3 weeks was detected protective effects [24], we observed that upregulation of autophagy by cardiac-specific beclin1 overexpression ameliorated cardiac systolic dysfunction at 2 weeks after MI. Unfortunately, we found that the improved post-infarct systolic dysfunction in beclin1 mice could not be maintained over time, and the post-infarct diastolic dysfunction also did not get better by cardiac-specific beclin1 overexpression. Instead, more fibrotic interstitial structure between myocardial fibers was found at the infarct border zone in beclin1 mice. Our and others results on fibroblasts have showed that upregulation of autophagy promotes the activation of cardiac fibroblasts to cardiac myofibroblasts as well as the proliferation and migration of cardiac fibroblasts [25,26]. It is well accepted that the activated cardiac myofibroblasts play a critical role in tissue repair after heart infarction. Also, the activation of relatively quiescent cardiac fibroblast to hypersynthetic myofibroblasts is the hallmark of cardiac fibrosis, which contributes to the inappropriate remodeling of the myocardial interstitium [27]. Therefore, it is likely that constitutive upregulation of autophagy in the setting of MI might be involved in the cardiac fibrosis possible due to the pro-survival nature of autophagy by which preventing myocardium injury in response to the ischemic stress. It should be noted that myocardial fibrosis after MI was also aggravated by beclin1 silencing or CQ, which might be the case that the aforementioned promotion of cardiomyocyte death by impairment of autophagy accelerated the myocardial scar formation caused by MI. No matter, controversial data exists on autophagy and cardiac fibrosis [25,26,28], and the underlying mechanisms by which autophagy regulates cardiac fibrosis is largely unknown. Given the highly dynamic process of autophagy in which either over- or under-activated autophagy flux could be detrimental, it might be more difficult and should be more careful to treat diseases by intervening autophagy.

Although the exact machinery by which dysregulated autophagy contributed to the cardiac remolding and heart failure is not yet clarified, it has become increasingly evident that autophagy-dependent cell death is involved in many cardiovascular pathological processes. Necroptosis has recently been recognized as an important form in autophagy-triggered cell death. It has been shown a combination of rapamycin and the glucocorticoid dexamethasone triggers necroptosis in acute lymphoblastic leukemia cells [29]. Many others demonstrated that autophagy is able to inhibit necroptosis in L929 cells, lymphocytes, or human cancer cells [30,31]. Here, we showed that myocardial ischemic damage induced by permanent coronary artery occlusion *in vivo* or OGD *in vitro* caused a sustained upregulation of RIP1 and RIP3. Of note, the increased expression of RIP1 and RIP3 was observed not only in ischemic core area (data not shown) but also in infarcted border myocardium, and the progressive upregulation of RIP1 and RIP3 in infarcted border zone of mice heart and in the OGD-treated H9C2 cells was correlated with the augmented necrotic cell death and progressive LV remodeling, cardiac dysfunction and heart failure in mice. In line with the upregulation of RIP1 and RIP3, MLKL was found to be translocated from cytoplasm to membrane in response to OGD challenge. Although the downstream pathway of RIP1 and RIP3 is incompletely understood, it has been suggested that activated MLKL by RIP3 localized to intracellular and plasma membranes is essential for necroptosis execution by disrupting membrane and killing the cell [14]. Certain previous studies also identified that necroptosis involving the RIP1-RIP3-MLKL axis was related to the ischemia-reperfusion injury in rodent rats and the heart failure in end-stage heart failure patients [32,33], confirming the functional relevance of necroptosis with the cardiac remolding as well as heart failure at the chronic stage after MI. More important, we found that inhibition of autophagy, not only by pharmacologically with CQ, but also genetically by beclin1 knockdown, upregulated the expression of RIP3 in the infarct heart and aggravated OGD-induced necrotic cardiomyocyte death in a RIP3-dependent manner, while, necrotic cardiomyocyte death induced by OGD could be mitigated by upregulation of autophagy through beclin1 overexpression. These results provided evidence that autophagy dysfunction was capable of activating, or might switch directly to necroptosis, thereby contributed to the progressive cardiac remolding and heart failure, although the exact molecular mechanisms by which autophagy dysfunction-mediated necroptosis is largely unknown and need to be further studied.

Actually, there is evidence that the levels of cardiomyocyte necrosis were sevenfold greater than apoptosis in the heart failure patients [34]. Necroptosis also has been reported to account for approximately 50% of cellular death as compared with 30% of apoptosis in the context of cardiac IR injury [35], suggesting that cardiac myocyte necrosis might be critical for the loss of cardiomyocyte and the development of heart failure. Our data supported this notion and showed that activation of necroptosis by RIP3 overexpression in cardiomyocytes aggravated the necrotic cardiomyocytes death induced by OGD. Importantly, constitutive activation of necroptosis by forced cardiac-specific overexpression of RIP3 increased myocardial infarction sizes and markedly worsen MI-induced myocardial injury as well as cardiac dysfunction. While, genetic inhibition of necroptosis by RIP3 knockdown supported the OGD-treated cardiomyocyte survival and could ameliorated cardiac remodeling and dysfunction. Consistent with our findings, Luedde M et al reported that RIP3 exerts negative effects on post-ischemic cardiac remodeling [36]. These results suggested that loss of cardiomyocyte by necroptosis might actively contribute not only to acute myocardial ischemic injury after MI but also to the progressive cardiac remolding and heart failure. Therefore, inhibition of necroptosis might be the potential target for preventing cardiac remodeling and heart failure.

In conclusion, in the present study, we highlighted that the proper autophagy is essential for the cardiac performance, while, autophagy dysfunction contributed to the adverse cardiac remodeling after myocardial infarction. We revealed that impairment of autophagy flux could mediate necroptosis, thereby contributed to the cardiomyocyte loss. Inhibition of necroptosis ameliorated MI-induced cardiac remodeling and dysfunction as well as the heart failure, thus, therapeutic inhibition of necroptosis may open new perspectives for the development of novel treatment approaches in cardiovascular diseases and heart failure.

CRediT author statement

Haining Zhang: Responsible for Project administration. **Yuan Yin, Yumei Liu and Hao Huang:** Conducting Investigation. **Gangling Zou and Guiping Zhang:** Data curation. **Peipei Qian and Jinxin Zhang:** Formal analysis. **Haining Zhang and Jinxin Zhang:** Writing - original

draft, Writing - review & editing. All authors provided comments on original draft and final manuscript. All authors approved the final version.

Declaration of Competing Interest

The authors declare that they have no known competing financial interests or personal relationships that could have appeared to influence the work reported in this paper.

Acknowledgements

This work was supported by Natural Science Foundation of Guangdong Province (No. 9151802002000001 and No. 2016A030313569 to H.N.Z), Science and Technology Program of Guangzhou (No. 201707010051 to H.N.Z) and Foundation of Guangzhou City Bureau of Education (10A179 to H.N.Z).

References

[1] J. Chen, A.F. Hsieh, K. Dharmarajan, F.A. Masoudi, H.M. Krumholz, National trends in heart failure hospitalization after acute myocardial infarction for Medicare beneficiaries: 1998–2010, Circulation 128 (24) (2013) 2577–2584.
[2] G.S. Bleumink, A.M. Knetsch, M.C. Sturkenboom, S.M. Straus, A. Hofman, J.W. Deckers, J.C. Witteman, B.H. Stricker, Quantifying the heart failure epidemic: prevalence, incidence rate, lifetime risk and prognosis of heart failure The Rotterdam Study, Eur. Heart J. 25 (18) (2004) 1614–1619.
[3] A. Nakai, O. Yamaguchi, T. Takeda, Y. Higuchi, S. Hikoso, M. Taniike, S. Omiya, I. Mizote, Y. Matsumura, M. Asahi, K. Nishida, M. Hori, N. Mizushima, K. Otsu, The role of autophagy in cardiomyocytes in the basal state and in response to hemodynamic stress, Nat. Med. 13 (5) (2007) 619–624.
[4] H.M. Shen, P. Codogno, Autophagic cell death: Loch Ness monster or endangered species? Autophagy 7 (5) (2011) 457–465.
[5] K. Nishida, M. Taneike, K. Otsu, The role of autophagic degradation in the heart, J. Mol. Cell. Cardiol. 78 (2015) 73–79.
[6] A. Shirakabe, P. Zhai, Y. Ikeda, T. Saito, Y. Maejima, C.P. Hsu, M. Nomura, K. Egashira, B. Levine, J. Sadoshima, Drp1-dependent mitochondrial autophagy plays a protective role against pressure overload-induced mitochondrial dysfunction and heart failure, Circulation 133 (13) (2016) 1249–1263.
[7] T. Saito, K. Asai, S. Sato, M. Hayashi, A. Adachi, Y. Sasaki, H. Takano, K. Mizuno, W. Shimizu, Autophagic vacuoles in cardiomyocytes of dilated cardiomyopathy with initially decompensated heart failure predict improved prognosis, Autophagy 12 (3) (2016) 579–587.
[8] S. Schlossarek, G. Mearini, L. Carrier, Cardiac myosin-binding protein C in hypertrophic cardiomyopathy: mechanisms and therapeutic opportunities, J. Mol. Cell. Cardiol. 50 (4) (2011) 613–620.
[9] G. Kung, K. Konstantinidis, R.N. Kitsis, Programmed necrosis, not apoptosis, in the heart, Circ. Res. 108 (8) (2011) 1017–1036.
[10] R.S. Whelan, V. Kaplinskiy, R.N. Kitsis, Cell death in the pathogenesis of heart disease: mechanisms and significance, Annu. Rev. Physiol. 72 (2010) 19–44.
[11] M. Chiong, Z.V. Wang, Z. Pedrozo, D.J. Cao, R. Troncoso, M. Ibacache, A. Criollo, A. Nemchenko, J.A. Hill, S. Lavandero, Cardiomyocyte death: mechanisms and translational implications, Cell Death Dis. 2 (12) (2011) e244.
[12] S. He, S. Huang, Z. Shen, Biomarkers for the detection of necroptosis, Cell. Mol. Life Sci. 73 (11–12) (2016) 2177–2181.
[13] Y.S. Cho, S. Challa, D. Moquin, R. Genga, T.D. Ray, M. Guildford, F.K. Chan, Phosphorylation-driven assembly of the RIP-RIP3 complex regulates programmed necrosis and virus induced inflammation, Cell 137 (6) (2009) 1112–1123.
[14] J.M. Murphy, P.E. Czabotar, J.M. Hildebrand, I.S. Lucet, J.G. Zhang, S. Alvarez-Diaz, R. Lewis, N. Lalaoui, D. Metcalf, A.I. Webb, S.N. Young, L.N. Varghese, G.M. Tannahill, E.C. Hatchell, I.J. Majewski, T. Okamoto, R.C. Dobson, D.J. Hilton, J.J. Babon, N.A. Nicola, A. Strasser, J. Silke, W.S. Alexander, The pseudokinase MLKL mediates necroptosis via a molecular switch mechanism, Immunity 39 (3) (2013) 443–453.
[15] H. Zhao, T. Jaffer, S. Eguchi, Z. Wang, A. Linkermann, D. Ma, Role of necroptosis in the pathogenesis of solid organ injury, Cell. Death Dis. (1975, 2015,) 6e.
[16] G.B. Koo, M.J. Morgan, D.G. Lee, W.J. Kim, J.H. Yoon, J.S. Koo, S.I. Kim, S.J. Kim, M.K. Son, S.S. Hong, J.M. Levy, D.A. Pollyea, C.T. Jordan, P. Yan, D. Frankhouser, D. Nicolet, K. Maharry, G. Marcucci, K.S. Choi, H. Cho, A. Thorburn, Y.S. Kim, Methylation-dependent loss of RIP3 expression in cancer represses programmed necrosis in response to chemotherapeutics, Cell Res. 25 (6) (2015) 707–725.
[17] A. Linkermann, M.J. Hackl, U. Kunzendorf, H. Walczak, S. Krautwald, A.M. Jevnikar, Necroptosis in immunity and ischemia-reperfusion injury, Am. J. Transplant. 13 (11) (2013) 2797–2804.
[18] Pingjun Zhu, Hu. Shunying, Qinhua Jin, Dandan Li, Feng Tian, Sam Toan, Yang Li, Hao Zhou, Yundai Chen, Ripk3 promotes ER stress-induced necroptosis in cardiac IR injury: a mechanism involving calcium overload/XO/ROS/mPTP pathway, Redox Biol. 16 (2018) 157–168.
[19] S.Y. Lim, S.M. Davidson, M.M. Mocanu, D.M. Yellon, C.C.T. Smith, The cardioprotective effect of necrostatin requires the cyclophilin-D component of the mitochondrial permeability transition pore, Cardiovasc. Drugs Ther. 21 (6) (2007) 467–469.
[20] L.T. Bish, H.L. Sweeney, O.J. Müller, R. Bekeredjian, Adeno-associated virus vector delivery to the heart, Methods Mol. Biol. 807 (2011) 219–237.
[21] Y. Lee, H.Y. Lee, A.B. Gustafsson, Regulation of autophagy by metabolic and stress signaling pathways in the heart, J. Cardiovasc. Pharmacol. 60 (2) (2012) 118–124.
[22] X. Ma, H. Liu, S.R. Foyil, R.J. Godar, C.J. Weinheimer, J.A. Hill, A. Diwan, Impaired autophagosome clearance contributes to cardiomyocyte death in ischemia/reperfusion injury, Circulation 125 (25) (2012) 3170–3181.
[23] Ting Gao, Shao-Ping Zhang, Jian-Fei Wang, Li Liu, Yin Wang, Zhi-Yong Cao, Hu. Qi-Kuan, Wen-Jun Yuan, Li Lin, TLR3 contributes to persistent autophagy and heart failure in mice after myocardial infarction, J. Cell. Mol. Med. 22 (1) (2018) 395–408.
[24] H. Kanamori, G. Takemura, K. Goto, R. Maruyama, K. Ono, K. Nagao, A. Tsujimoto, A. Ogino, T. Takeyama, T. Kawaguchi, T. Watanabe, M. Kawasaki, T. Fujiwara, H. Fujiwara, M. Seishima, S. Minatoguchi, Autophagy limits acute myocardial infarction induced by permanent coronary artery occlusion, Am. J. Physiol. Heart Circ. Physiol. 300 (6) (2011) H:2261–H:2271.
[25] S.S. Gupta, M.R. Zeglinski, S.G. Rattan, N.M. Landry, S. Ghavami, J.T. Wigle, T. Klonisch, A.J. Halayko, I.M. Dixon, Inhibition of autophagy inhibits the conversion of cardiac fibroblasts to cardiac myofibroblasts, Oncotarget 7 (48) (2016) 78516–78531.
[26] Gangling Zou, Yumei Liu, Haining Zhang, Effect of autophagy on Ang II-induced proliferation and migration of cardiac fibroblasts, J. Guangdong Pharmaceut. Univ. 31 (3) (2015) 407–411 (in Chinese).
[27] J.D. Lajiness, S.J. Conway, Origin, development, and differentiation of cardiac fibroblasts, J. Mol. Cell. Cardiol. 70 (2014) 2–8.
[28] R.N. Wu, T.Y. Yu, J.C. Zhou, M. Li, H.K. Gao, C. Zhao, R.Q. Dong, D. Peng, Z.W. Hu, X.W. Zhang, Y.Q. Wu, Targeting HMGB1 ameliorates cardiac fibrosis through restoring TLR2-mediated autophagy suppression in myocardial fibroblasts, Int. J. Cardiol. 267 (2018) 156–162.
[29] L. Bonapace, B.C. Bornhauser, M. Schmitz, G. Cario, U. Ziegler, F.K. Niggli, B.W. Schäfer, M. Schrappe, M. Stanulla, J.P. Bourquin, Induction of autophagy-dependent necroptosis is required for childhood acute lymphoblastic leukemia cells to overcome glucocorticoid resistance, J. Clin. Investig. 120 (4) (2010) 1310–1323.
[30] T. Farkas, M. Daugaard, M. Jaattela, Identification of small molecule inhibitors of phosphatidylinositol 3-kinase and autophagy, J. Biol. Chem. 286 (45) (2011) 38904–38912.
[31] Y.C. Ye, L. Yu, H.J. Wang, S. Tashiro, S. Onodera, T. Ikejima, TNFα-induced necroptosis and autophagy via supression of the p38-NF-κB survival pathway in L929 cells, J. Pharmacol. Sci. 117 (3) (2011) 160–169.
[32] Adrián Szobi, Veronika Farkašová-Ledvényiová, Martin Lichý, Martina Muráriková, Slávka Čarnická, Tatiana Ravingerová, Adriana Adameová, Cardioprotection of ischaemic preconditioning is associated with inhibition of translocation of MLKLwithin the plasma membrane, J. Cell. Mol. Med. 22 (9) (2018) 4183–4196.
[33] Adrián Szobi, Eva Gonçalvesová, Zoltán Varga, Przemyslaw Leszek, Mariusz Kuśmierczyk, Michal Hulman, Ján Kyselovič, Péter Ferdinandy, Adriana Adameová, Analysis of necroptotic proteins in failing human hearts, J. Transl. Med. 15 (1) (2017) 86.
[34] S. Guerra, A. Leri, X. Wang, N. Finato, C. Di Loreto, C.A. Beltrami, J. Kajstura, P. Anversa, Myocyte death in the failing human heart is gender dependent, Circ. Res. 85 (9) (1999) 856–866.
[35] T. Zhang, Y. Zhang, M. Cui, L. Jin, Y. Wang, F. Lv, Y. Liu, W. Zheng, H. Shang, J. Zhang, M. Zhang, H. Wu, J. Guo, X. Zhang, X. Hu, C.M. Cao, R.P. Xiao, CaMKII is a RIP3 substrate mediating ischemia- and oxidative stress-induced myocardial necroptosis, Nat. Med. 22 (2) (2016) 175–182.
[36] M. Luedde, M. Lutz, N. Carter, J. Sosna, C. Jacoby, M. Vucur, J. Gautheron, C. Roderburg, N. Borg, F. Reisinger, H.J. Hippe, A. Linkermann, M.J. Wolf, S. Rose-John, R. Lüllmann-Rauch, D. Adam, U. Flögel, M. Heikenwalder, T. Luedde, N. Frey, RIP3, a kinase promoting necroptotic cell death, mediates adverse remodelling after myocardial infarction, Cardiovasc. Res. 103 (2) (2014) 206–216.